

In-Situ Characterization of Deformation and Fracture Behavior of Hot-Rolled Medium Manganese Lightweight Steel

ZHENG-ZHI ZHAO,¹ RONG-HUA CAO,¹ JU-HUA LIANG,¹ FENG LI,¹
CHENG LI,¹ and SHU-FENG YANG^{2,3}

1.—Collaborative Innovation Center of Steel Technology, University of Science and Technology Beijing, Beijing 100083, China. 2.—School of Metallurgical and Ecological Engineering, University of Science and Technology Beijing, Beijing 100083, China. 3.—e-mail: yangshufeng_ustb@126.com

The deformation and fracture behavior of hot-rolled medium manganese lightweight (0.32C-3.85Mn-4.18Al-1.53Si) steel was revealed by an in situ tensile test. Deformed δ -ferrite with plenty of cross-parallel deformation bands during in situ tensile tests provides δ -ferrite of good plasticity and ductility, although it is finally featured by the cleavage fracture. The soft and ductile δ -ferrite and high-volume fraction of austenite contribute to the superior mechanical properties of medium manganese lightweight steel heated at 800°C, with a tensile strength of 924 MPa, total elongation of 35.2% and product of the strength and elongation of 32.5 GPa %.

INTRODUCTION

Advanced lightweight automotive steels, with an excellent combination of strength and ductility, meet energy-saving and environmental protection needs.¹ Due to its excellent mechanical properties, low material cost and industrial feasibility, medium manganese lightweight steel with Mn content of 3–10% has become a candidate material for automobile steel and has promising prospects.^{2,3} The excellent mechanical properties of medium manganese steel are mainly attributed to the phase transformation-induced plasticity (TRIP) effect of austenite, usually obtained by intercritical annealing.^{1–4} The TRIP effect of austenite leads to work hardening, thus delaying the start of necking and significantly improving the tensile properties of steel. In addition, Al in lightweight steel not only promotes the growth of intercritical ferrite,^{5,6} but also keeps δ -ferrite at room temperature during solidification. The existence of δ -ferrite facilitates partitioning of alloying elements to austenite, thereby increasing its stability. Thus, it can improve the tensile properties of steels.^{1,7}

Recently, researchers have focused on ways to improve the mechanical properties of medium manganese lightweight steel,^{3,8–10} while there are few studies on the fracture behavior of medium manganese lightweight steel. In this article, the

deformation behavior of the microstructure and fracture morphology is carefully observed by both offline and in situ tensile testing.

EXPERIMENTAL PROCEDURE

The experimental steel with a composition (wt.%) of C 0.32, Si 1.53, Mn 3.85, Al 4.18, P 0.007 and S 0.017, Fe bal., was prepared using a vacuum furnace and forged into slabs with dimensions of 40 mm × 70 mm × 100 mm. The forged slabs were then reheated to 1200°C for 1 h and hot-rolled to a 4-mm-thick (~90% reduction) plate after five passes, finished at 900°C, followed by air cooling to room temperature. Rectangular samples of 20 mm × 100 mm were cut on the hot-rolled sheet and heated at 750°C, 800°C, and 850°C for 8.5 min in a box-type resistance furnace and then water quenched to room temperature.

Microstructures were observed using Zeiss ULTRA 55-type field emission scanning electron microscopy (FE-SEM) after etching with 2% nitric acid alcohol. Electron backscatter diffraction (EBSD) was performed on the samples with 20 kV and a step size of 0.3 μ m. The surfaces of the samples for EBSD and XRD were electrolytically polished with a negligible internal stress in a mixture reagent of 20% perchloric acid and 80% ethanol with voltage of 15 V for 20 s. The in situ

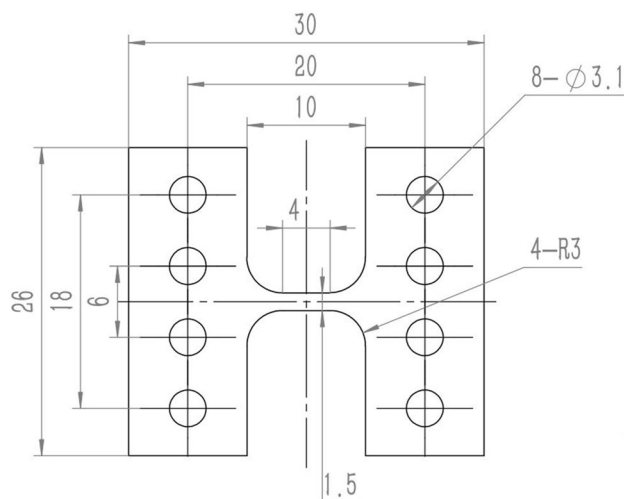


Fig. 1. Schematic of the in situ tensile specimen.

tensile test was also operated in an ULTRA 55 thermal field emission scanning electron microscope. The in situ tensile specimen, shown in Fig. 1 (unit:mm), was first electrolytically polished with a negligible internal stress and then eroded. Tensile specimens with a gauge length of 25 mm and thickness of 3 mm with the oxide layer removed were cut along the rolling direction for room-temperature uniaxial tensile tests at a rate of $1 \text{ mm}\cdot\text{min}^{-1}$. The elongation of the steel was tested twice and then averaged. The hardness values were measured five times for each phase with a load of 50 g and maintained 10 s using a micro-Vickers hardness tester and then averaged.

RESULTS AND DISCUSSION

Microstructure and Mechanical Properties

The hot-rolled microstructure contains δ -ferrite (δ), martensite (M) and a small amount of fine equiaxed ferrite (F), as shown in Fig. 2a. The banded martensite and δ -ferrite are distributed alternately along the rolling direction, and fine equiaxed ferrite is precipitated along the deformed prior austenite grain boundaries during the hot-rolling and subsequent cooling. After the following heat treatment, banded microstructures (Fig. 2) of samples heated at different temperatures inherit from the hot-rolled banded microstructure. Correspondingly, the microstructure is composed of banded δ -ferrite, lath-like ultra-fine grained (UFG) intercritical ferrite (IF), austenite (A), martensite and carbides. The carbides are only observed in samples heated at the lowest temperature of 750°C . The highest austenite fraction has been detected in the sample heated at 800°C by both the EBSD (Fig. 2e) and XRD (Fig. 3) technique, and no martensite transformation occurs during quenching. With rising temperature, thermally transformed martensite exists in the sample heated at 850°C , resulting in the lower austenite fraction at room temperature (Fig. 3).

The detailed mechanical properties are shown in Fig. 4. The increasing ultimate tensile strength (UTS) with the rising heating temperature results from the increasing martensite fraction both thermally transformed from the intercritical austenite and mechanically induced. Besides, the decline of yield strength (YS) mainly comes from the coarse grains, especially the coarse δ -ferrite, because of the rising temperature.

The total elongation (TE) increases with the increasing annealing temperature and then decreases. This is considered mainly related to the intercritical ferrite volume fraction and austenite volume fraction and stability. The TE of the specimen annealed at 800°C is as high as 35.2%, which was much larger than the TEs of the specimen annealed at 750°C and 850°C . The lowest TE of the specimen annealed at 850°C is likely attributed to the higher proportion of thermally transformed martensite. It is easy to understand that the intercritical austenite heated at a higher temperature has a lower thermal stabilization due to the low average alloy content. Thus, fresh martensite in the sample heated at 850°C exacerbated its elongation.

It is noteworthy that the sample heated at 750°C and 800°C exhibits the necking, while there is no necking of the sample heated at 850°C . The PUE decreases as a function of heating temperature, as shown in Fig. 4b. Thus, the fracture morphology is further observed, as shown in Fig. 5.

Fracture Morphology

The corresponding fracture characteristics of the necking of the sample heated at 750°C is found. Plenty of micro-cracks are observed in the sample heated at 750°C (Fig. 5b). However only a few large micro-cracks are observed in the sample heated at 850°C (Fig. 5f), indicating its rapid crack propagation, which accounts for why necking did not occur.

Fracture morphology is closely related to the deformed microstructure.¹¹ Based on the size and morphology of each phase, there are obvious river patterns in the fracture (Fig. 5a) corresponding to the δ -ferrite (Fig. 5b). Similar fracture features of δ -ferrite have also been reported in related literature.¹² By contrast, there are plenty of dimples in the UFG ferrite and austenite region. Micro-cracks easily nucleate near the carbide particles.¹³ Although carbide particles hinder the movement of dislocation to improve the strength of steel, the formation of carbide-induced layer micro-cracks easily grow together to form cracks, which seriously undermine the plasticity of steel. In addition, a long crack along the δ -ferrite and intercritical ferrite and austenite interfacial layer can be observed in the fracture, and inclusions are found in the long crack (marked by the red arrow). Meanwhile, a corresponding crack is also found in Fig. 5b. Choi et al.¹⁴ consider that long cracks are not the cause of fractures, but caused by fractures.

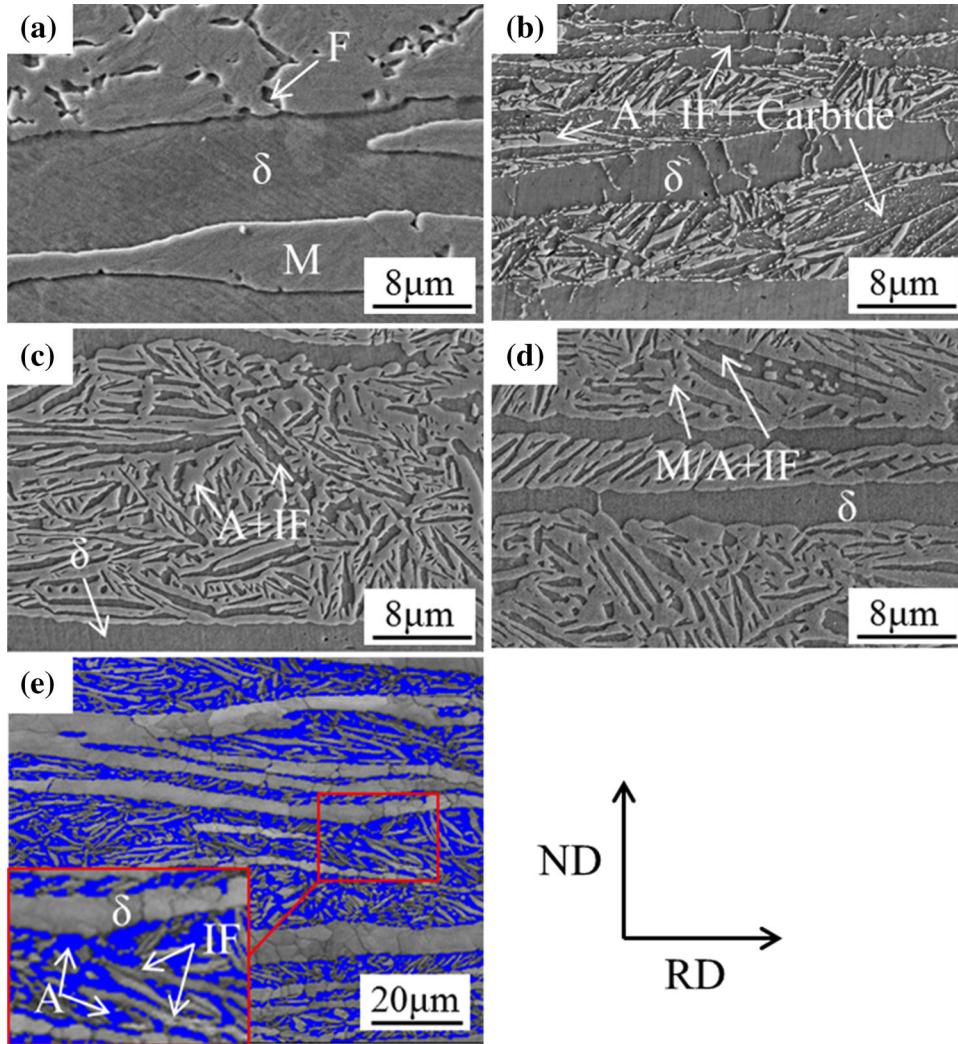


Fig. 2. SEM micrographs of the experimental steel (a) in the as-hot rolled condition, heated at (b) 750°C, (c) 800°C, and (d) 850°C. (e) EBSD map of sample heated at 800°C; blue regions denote austenite (Color figure online).

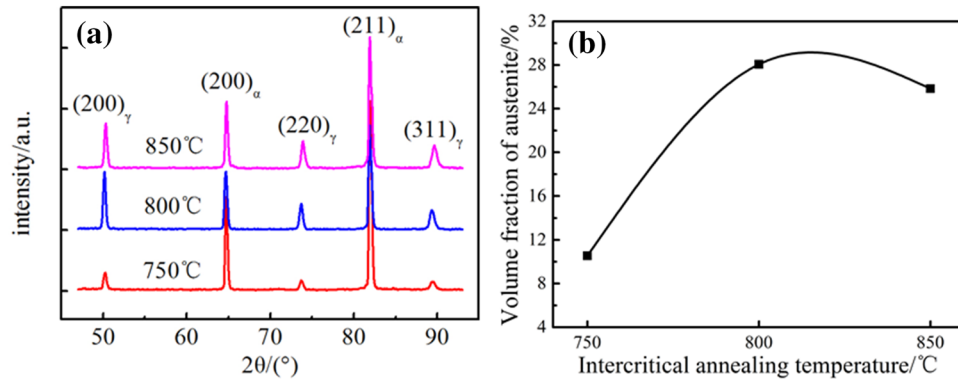


Fig. 3. XRD patterns and measured austenite fractions of Fe-0.32C-3.85Mn-4.18Al-1.53Si steel annealed at different temperatures. (a) XRD patterns. (b) The measured austenite volume fractions.

A similar cleavage fracture of δ -ferrite is also observed in the sample heated at 800°C and 850°C, while distinctly different fracture characteristics are

observed in the mixed zone of UFG ferrite and martensite or austenite. The sample annealed at 800°C exhibits ductile fracture characteristics with

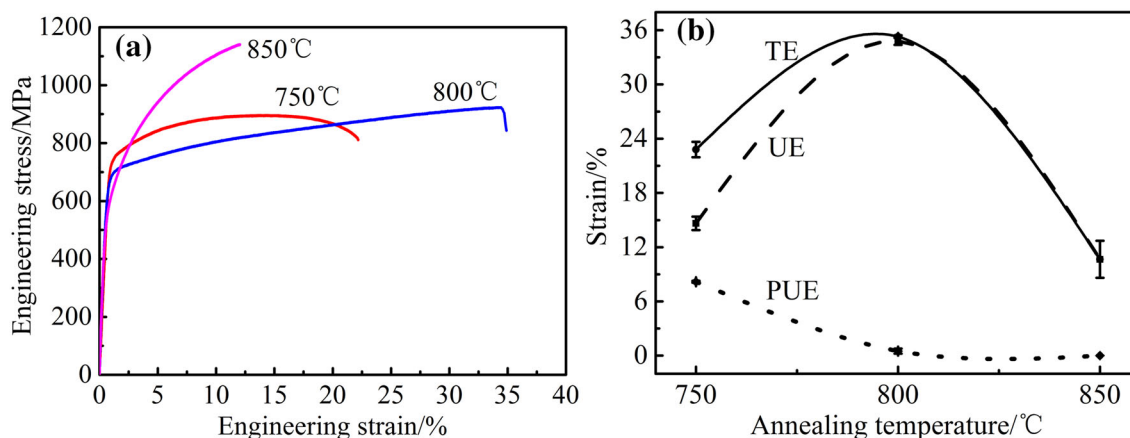


Fig. 4. (a) Engineering stress–strain curves and (b) the annealing temperature dependence of total elongation (TE), uniform elongation (UE), and post-uniform elongation (PUE).

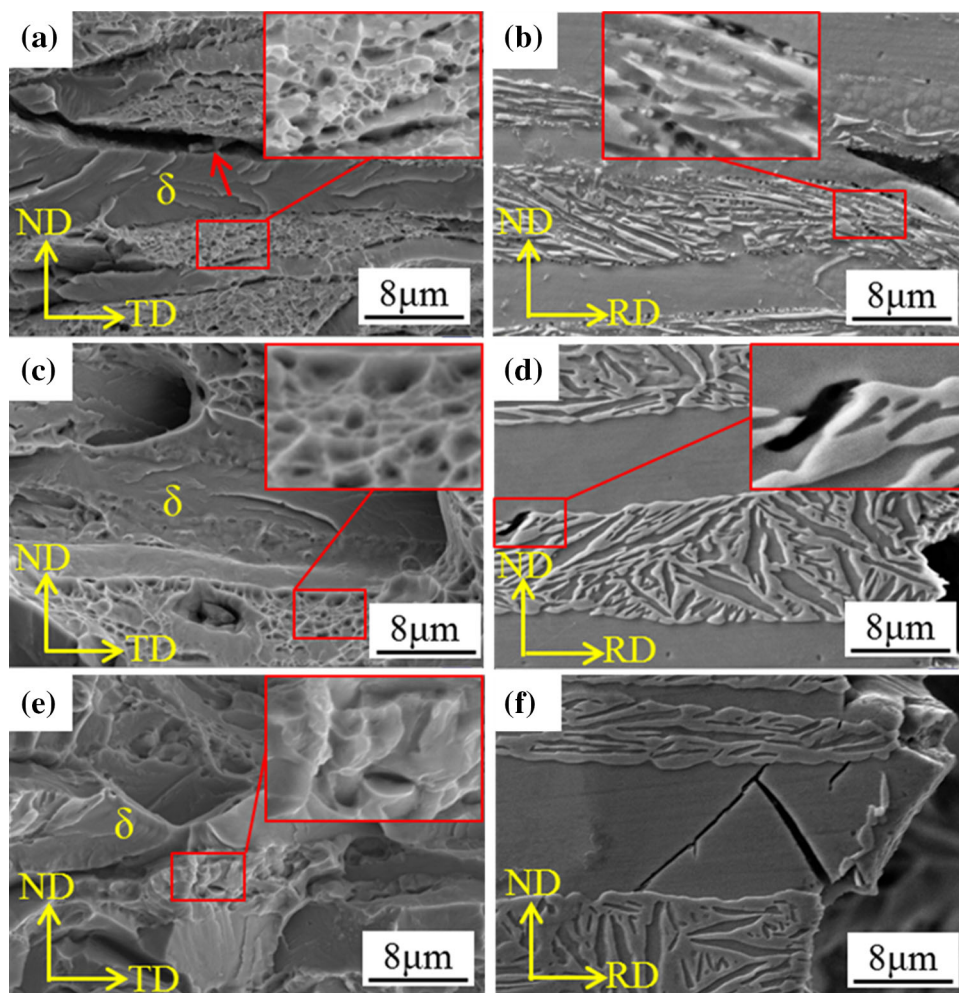


Fig. 5. (a, c, and e) Fracture morphologies and (b, d, and f) the deformed microstructure near the fracture of Fe-0.32C-3.85Mn-4.18Al-1.53Si steel after tensile deformation. Annealing temperatures: (a, b) 750°C, (c, d) 800°C, and (e, f) 850°C.

distinct dimples, whereas the sample annealed at 850°C exhibits quasi-cleavage fracture characteristics in the mixed zone, consistent with its poor elongation.

Figure 5d shows that there is only one micro-crack at the interface between the intercritical ferrite and the strain-induced martensite of the sample heated at 800°C due to the different deformation characteristics of the

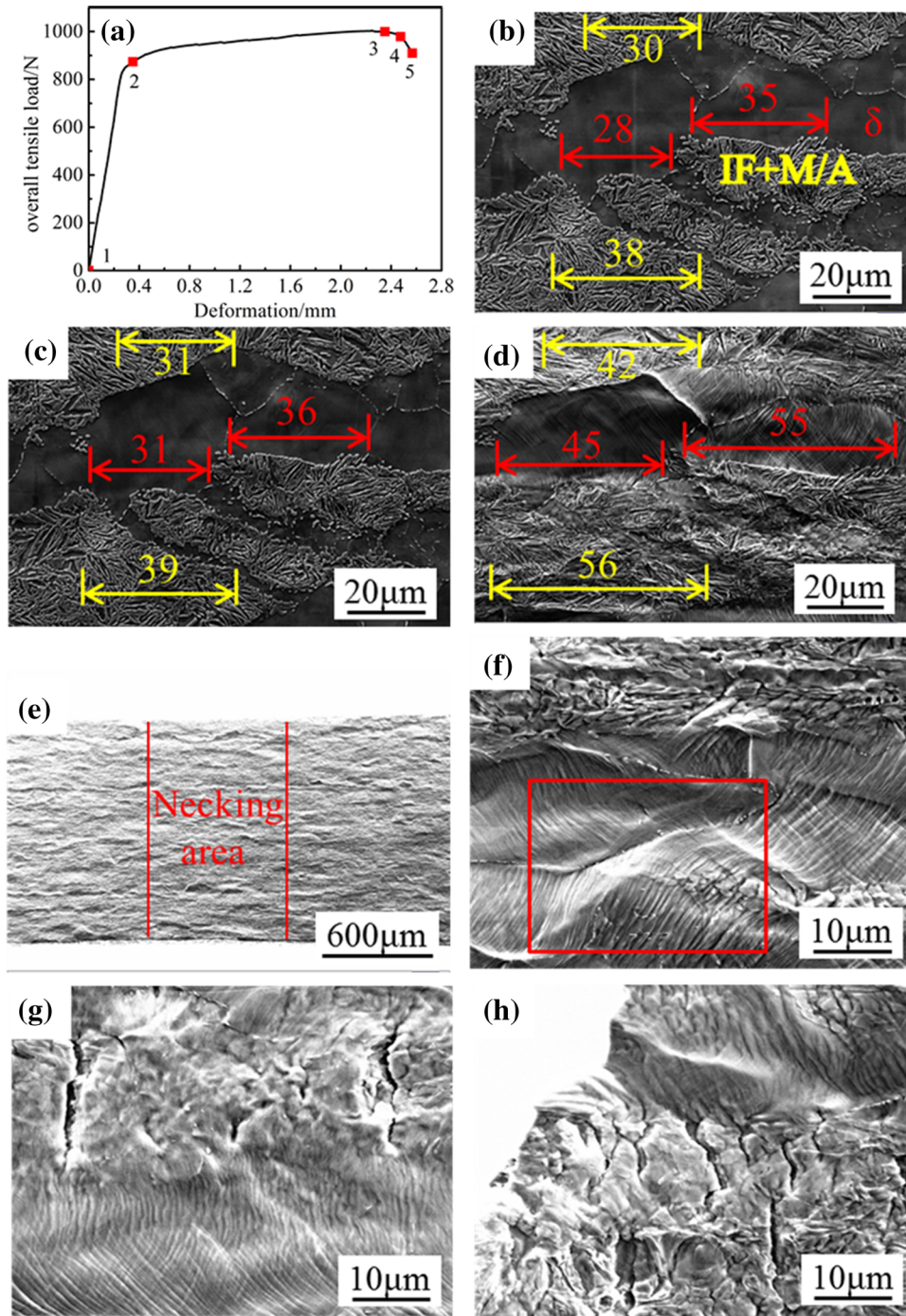


Fig. 6. In-situ tensile curve of the sample heated at 800°C. (a) Microstructure under uniform deformation stage. (b) Point 1, (c) point 2, and (d) point 3, embedded by real-time phase lengths (μm). Microstructure of the necking area under the post-uniform deformation stage, corresponding to (e, f, g) point 4 and microstructure near the fracture after failure of (h) point 5.

two phases. The intercritical ferrite is the soft phase, and martensite is the hard phase, which means the strain of martensite is smaller than that of intercritical ferrite, resulting in a large strain gradient at the interface and contributing to easy nucleation of micro-cracks here.¹⁵

As shown in Fig. 5f, several micro-cracks are observed in δ -ferrite of the sample heated at 850°C, which may be attributed to the formation of deformed twins in δ -ferrite that provide nucleation sites for micro-cracks during deformation.^{12,16}

In-Situ Tensile Tests Analysis

The microstructures at different stages in the in situ tensile curve of the sample heated at 800°C during the in situ tensile test are shown in Fig. 6. When the deformation increased from 0 mm to 2.35 mm, both coarse δ -ferrite and the mixed phase of UFG intercritical ferrite and austenite were elongated along the tensile direction by $59 \pm 2\%$ and $44 \pm 4\%$, respectively. This result implies that there is an inhomogeneous strain distribution between δ -ferrite and the mixed phase. The δ -ferrite deforms at a higher rate than the mixed phase, and it is also consistent with hardness because the hardness value of δ -ferrite ($HV290 \pm 9$) is lower than that of the mixed phase ($HV309 \pm 10$). From the tensile deformation fracture morphology (Fig. 5-c) of the specimen heated at 800°C, it is observed that the δ -ferrite phase shows a complete cleavage fracture, while the fracture surfaces of the mixed phase present dimple behavior. Therefore, it is inaccurate to use the fracture surface to simply determine the ductility and brittleness of the material.

The heavily deformed δ -ferrite produces a large number of cross-parallel deformation bands, especially in the post-uniform deformed microstructure after necking. And the deformed δ -ferrite revealed rugged surfaces (marked by red rectangles). This also implies that the δ -ferrite is soft and in the ductile phase, and it can sustain greater deformation, thus contributing to the ductility of experimental steel.

In the post-uniform deformation stage (Fig. 6f and g), nucleation and growth of the micro-cracks perpendicular to the tensile direction occurred first in the mixed phase of UFG intercritical ferrite and were retained. Cracks are not found in δ -ferrite. When the loading continues, the specimen instantly breaks (Fig. 6h), and no cracks perpendicular to the tensile direction are observed in the δ -ferrite. This indicates that as soon as the micro-crack perpendicular to the tensile direction nucleates in δ -ferrite, the tensile specimens immediately fracture. Thus, there will be no crack diffusion in δ -ferrite. This is probably attributed to the fact that δ -ferrite with good plasticity and ductility suffers severe deformation and work hardening. The δ -ferrite in this moment must have high dislocation density and a large number of deformation bands, allowing the rapid propagation of cracks along these deformation bands, and accounts for the cleavage fracture in Fig. 5. Thus, δ -ferrite suffering severe deformation may easily be mistaken for a brittle phase.

CONCLUSION

- (1) The specimen annealed at 800°C with a microstructure consisting of an UFG intercritical ferrite, austenite and coarse-grained δ -ferrite exhibits an excellent combination of UTS of 924 MPa, TE of 35.2% and UTS \times TE of 32.5 GPa %.
- (2) Fracture morphology of a large number of micro-cracks nucleated at the carbide is consistent with the outstanding necking of the sample heated at 750°C. The thermally transformed fresh martensite in the sample heated at 850°C results in its engineering stress-strain curves with no necking.
- (3) Deformed δ -ferrite with a large number of cross-parallel deformation bands revealed by the in situ tensile test proves the δ -ferrite is of good plasticity and ductility, although it is finally featured by the cleavage fracture.

ACKNOWLEDGEMENTS

Zhengzhi Zhao acknowledges the financial support from the National Natural Science Foundation of China (No. 51574028).

REFERENCES

1. Z.H. Cai, H. Ding, R.D.K. Misr, and Z.Y. Ying, *Acta Mater.* 84, 229 (2015).
2. C.-Y. Lee, J. Jeong, J. Han, S.-J. Lee, S. Lee, and Y.-K. Lee, *Acta Mater.* 84, 1 (2014).
3. C.W. Shao, W.J. Hui, Y.J. Zhang, X.L. Zhao, and Y.Q. Weng, *Mater. Sci. Eng. A* 682, 45 (2017).
4. S. Lee and B.C. De Cooman, *Metall. Mater. Trans. A* 44, 5018 (2013).
5. D.W. Suh, S.J. Park, C.S. Oh, and S.J. Kim, *Scr. Mater.* 57, 1097 (2007).
6. T. Bhattacharyya, S.B. Singh, S. Das, A. Haldar, and D. Bhattacharjee, *Mater. Sci. Eng. A* 528, 2394 (2011).
7. H.L. Yi, S.K. Ghosh, W.J. Liu, K.Y. Lee, and H.K.D.H. Bhadeshia, *Mater. Sci. Technol.* 26, 817 (2010).
8. C.-H. Seo, K.H. Kwon, K. Choi, K.-H. Kim, J.H. Kwak, S. Lee, and N.J. Kim, *Scr. Mater.* 66, 519 (2012).
9. S.J. Park, B. Hwang, K.H. Lee, T.H. Lee, D.W. Suh, and H.N. Han, *Scr. Mater.* 68, 365 (2013).
10. S. Lee, S. Shin, M. Kwon, K. Lee, and B.C. De Cooman, *Metall. Mater. Trans. A* 48, 1678 (2017).
11. J. Liang, Z. Zhao, D. Tang, N. Ye, S. Yang, and W. Liu, *Mater. Sci. Eng. A* 711, 175 (2018).
12. B. Sun, F. Fazeli, C. Scott, X. Yan, Z. Liu, X. Qin, and S. Yue, *Scr. Mater.* 130, 49 (2017).
13. J. Kadkhodapour, A. Butz, and S. Ziaei Rad, *Acta Mater.* 59, 2575 (2011).
14. H. Choi, S. Lee, F. Barlat, and B.C. De Cooman, *Mater. Sci. Eng. A* 687, 200 (2017).
15. G. Avramovic-Cingara, ChAR Saleh, M.K. Jain, and D.S. Wilkinson, *Mater. Trans. A* 40, 3117 (2009).
16. T. Šmida and J. Bošanský, *Mater. Sci. Eng. A* 287, 107 (2000).